Phase Behavior of Blends of Linear and Branched Polyethylenes on Micron Length Scales via Ultra-Small-Angle Neutron Scattering

M. Agamalian,*,† R. G. Alamo,‡ M. H. Kim,‡ J. D. Londono,†,§ L. Mandelkern,⊥ and G. D. Wignall†

Solid State Division, Oak Ridge National Laboratory,# Oak Ridge, Tennessee 37830-6393; Department of Chemical Engineering, Florida Agricultural and Mechanical University and Florida State University College of Engineering, Tallahassee, Florida 32310; and Institute of Molecular Bio-physics, Florida State University, Tallahassee, Florida 32306

Received July 13, 1998; Revised Manuscript Received October 27, 1998

ABSTRACT: Small-angle neutron scattering (SANS) experiments have indicated that mixtures of linear (high density) and long chain branched (low density) polyethylenes (HDPE/LDPE) form a one-phase mixture in the melt. However, the maximum spatial resolution of pinhole SANS cameras is $\sim 10^3$ Å, and it has been suggested that such experiments do not provide unambiguous evidence for a homogeneous melt. Thus, the SANS data might also be interpreted as arising from a biphasic melt with a very large particle size ($\sim 3\ \mu$m), because most of the scattering from the different phases would not be resolved. We have addressed this hypothesis by means of ultra-small-angle neutron scattering (USANS) experiments, using a newly developed Bonse-Hart USANS facility, which can resolve particle dimensions up to 30 μm. The experiments confirm that HDPE/LDPE blends are homogeneous in the melt on length scales probed by pinhole SANS and also by USANS. We have also studied blends of linear and short-chain branched polyethylenes, which phase separate when the branch content is sufficiently high. It is shown that USANS can directly resolve both the size of the dispersed phase ($\sim 4\ \mu$m) and the forward cross section [$d\Sigma/d\Omega(0) \sim 10^8$ cm^{-1}], which is 6 orders of magnitude higher than for homogeneous blends.

Introduction

Polyethylene (PE) is produced in many forms, each of which has different properties resulting from variations in structure. High-density PE (HDPE) is the most crystalline form, because the chains contain very little branching. Typical low-density PEs (LDPE) contain short-chain branches (1−3 per 100 backbone carbon atoms) as well as long-chain branches (0.1−0.3 per 100 backbone carbon atoms). Linear low-density PE (LLDPE) is produced by copolymerizing ethylene with an α-olefin such as hexene and can have a wide range of branch contents, depending on the catalyst and concentration of added comonomer. The properties of the individual species can be altered by mixing the components, and blends of HDPE, LDPE, and LLDPE are widely used commercially. However, understanding of the mechanical and melt flow properties of such blends is handicapped by the absence of a consensus concerning the melt miscibility of the components. For example, different views have been expressed in the literature ranging from liquid−liquid phase segregation[2,5−7] to complete homogeneity in the melt[1,4,8,9] for HDPE/LDPE mixtures. SANS can supply information on melt homogeneity of polymer blends via the contrast achieved by deuteration, and this technique has been used extensively to study the melt compatibility,[1,4,10] solid-state morphology,[11] and thermodynamics[12−18] of mixtures of linear and branched polyolefins, including HD, LD, and LLDPEs.

Pinhole SANS data, with a resolution limit $\sim 10^3$ Å, indicate that for HDPE/LDPE blends with molecular weights $\sim 10^5$ the melt is homogeneous,[1] after accounting for H/D isotope effects.[19−21] Similarly, mixtures of HDPE and LLDPE are homogeneous in the melt[4] when the branch content is low (i.e., <4 branches/100 backbone carbons). However, when the branch content is high (>8 branches/100 backbone carbons), the blends phase separate.[4] It has been asserted[2] that these experiments do not provide unambiguous evidence for a one-phase (homogeneous) melt for HDPE/LDPE blends and that the data might also be interpreted as arising from a biphasic melt with a very large particle size. Previous experiments[1,4] were performed with a minimum value of the momentum transfer, $Q = 4\pi\lambda^{-1} \sin\theta \sim 0.004$ Å^{-1} (where λ is the wavelength and 2θ is the angle of scatter), so the maximum spatial resolution is therefore $D \sim 2\pi/Q_{min} \sim 1500$ Å. Thus, if the domains had micron-size dimensions, much of the scattering from the dispersed phase would be exhibited at Q values $<10^{-3}$ Å^{-1}.

We have addressed this hypothesis via a new ultra-high-resolution (USANS) instrument,[3] which increases the spatial resolution to $D = 2\pi/Q_{min} \sim 30\ \mu$m, and it will be seen that these experiments demonstrate that the phase-separated blend has an extremely high [$d\Sigma/d\Omega(Q) \sim 10^8$ cm^{-1}] cross section at $Q \sim 10^{-5}$ Å^{-1}. Conversely, the USANS signal from the homogeneous blend of HDPE/LDPE is virtually indistinguishable from the unlabeled LDPE homopolymer "blank", which is to be expected if the blend is homogeneous as concluded previously from pinhole SANS data.[1,4]

Experimental Section

Materials and Sample Preparation. The polyethylenes used are identical or very similar to those used in previous work,[1,4] and their molecular characteristics are given in Table 1, using the same nomenclature for the polymer components

* Corresponding author.
† Oak Ridge National Laboratory.
‡ Florida Agricultural and Mechanical University and Florida State University College of Engineering.
⊥ Institute of Molecular Biophysics, Florida State University.
§ Current address: DuPont Central Research and Development Experimental Station, Building E323, P.O. Box 80323, Wilmington, Delaware 19880-0323.
# Managed by Lockheed Martin Energy Research Corp. under Contract DE-AC05-84OR2140 for the U.S. Department of Energy.

10.1021/ma981091b CCC: $18.00
Published on Web 04/09/1999

Table 1. Molecular Weights, Polydispersities, and Branch Content of Blend Component

	$10^{-3}M_w$	M_w/M_n	branches/100 backbone carbons: long[a]	branches/100 backbone carbons: short[b]
Hydrogenated Low-Density PE				
LDPE-3H	136	11.0	0.28	1.31
Hydrogenated Polybutadiene				
HPB-H35	78	1.1		10.6[c]
Hydrogenated High-Density PE				
HDPE-1	149	3.6		
Deuterated High-Density PE				
HDPE-4D	115.4	5.4		

[a] Branches containing >8 carbon atoms. [b] Branches containing ≤8 carbon atoms. [c] Ethyl branches.

as in previous publications.[1,4] Two blends that have already been studied by conventional pinhole SANS were remeasured with sample dimensions suitable for the USANS experiment, which uses a bigger beam cross-section area (2 × 4 cm^2) than for SANS (~1 cm diameter). A 75/25 blend of protonated LDPE (LDPE-3H) and deuterated HDPE (HDPE-4D) was prepared and would be expected to be homogeneous in the melt, based on previous SANS experiments. As an example of a phase-separated blend,[3] a 75/25 mixture of a highly branched hydrogenated polybutadiene (HPB-H35 with 10.6 mol % of ethyl branches) and linear PE was also prepared. HPB serves as a virtually monodisperse model LLDPE. The blends of branched and linear PEs were made by dissolving the initial components in 300 mL of *o*-dichlorobenzene (total weight 1.5 g) and stirring at 178 °C for 20 min. The solution was rapidly quenched into 3 L of chilled methanol (−50 °C), and after filtering and washing with methanol the crystals were dried in a vacuum oven at 60 °C. Rectangular plates with dimensions 2 cm × 4 cm × 0.15 cm were obtained via compression molding in a Carver press at 190 °C and quenched into ice water. As the phase-separated blend was expected to display a very high scattering cross section, only a fraction of the linear polymer was deuterated, and the percentages of each component in this blend were as follows: 75% of hydrogenated polybutadiene, HPB-H35; 15% of linear protonated, HDPE-1; and 10% of linear deuterated PE, HDPE-4D. By contrast, the amount of deuterated material (25%) was 2.5 times higher in the HDPE/LDPE blend to enhance the scattering from any morphological features present.

Neutron Scattering. Pinhole SANS data were collected on the W.C. Koehler 30m SANS facility[21] at the Oak Ridge National Laboratory via a 64 × 64 cm^2 area detector with the cell size ~1 cm^2 and the sample-to-detector distances of 10 and 19 m. The beam stop size (diameter) was 4 cm, and the wavelength, λ, was 4.75 Å. The data were collected on a cell-by-cell basis for the efficiency variation of the detector, instrumental (beam blocked) background, and also the intensities of the corresponding sample cells with quartz windows, which formed only a minor perturbation. The net intensities were converted to an absolute (±3%) differential cross section per unit sample volume [$d\Sigma/d\Omega(Q)$ in units of cm^{-1}] by comparison with precalibrated secondary standards[23] and radially averaged to give a Q range of $1.5 \times 10^{-3} < Q < 6 \times 10^{-2}$ Å^{-1}. Further details of data collection and correction procedure for incoherent scattering have been given previously.[1,4,24,25]

The USANS measurements were carried out on a Bonse-Hart double-crystal diffractometer (Figure 1) equipped by triple-bounce Si(111) channel-cut crystals, which have been modified by cutting an additional groove for a cadmium absorber.[3] This reduces the intensity of the wings of the rocking curve and improves the signal-to-noise ratio by 3 orders of magnitude, thus allowing the determination of phase dimensions up to ~30 μm, which corresponds to the lowest achievable value of $Q_{min} \sim 2 \times 10^{-5}$ Å^{-1}. In a USANS experiment (Figure 1) the beam is defined by Bragg reflection [$2\theta_B$ = 48.8° for Si(111)] from the triple-bounce channel-cut monochromator crystal and then enters a similar analyzer, which is scanned through a range of angles to measure the intensity as a function of Q. When a sample is placed between the analyzer and monochromator, small-angle scattering "spreads" the beam and is reflected in the excess intensity observed for $Q > 2 \times 10^{-5}$ Å^{-1}. The actual Q value at which the excess intensity scattered by the sample can be resolved from the "empty cell" scan with reasonable signal-to-noise ratio depends on the sample scattering cross section, and thus in our experiment the practical Q range was $3 \times 10^{-5} < Q < 2 \times 10^{-3}$ Å^{-1}. The data at each angle were normalized via the neutron beam monitor to correct for drifts in the incident beam intensity. After subtracting the instrumental backgrounds, the net intensities were normalized by the sample thickness and transmission coefficient, which is largely determined by the incoherent component of total scattering cross section. This parameter was measured by the monitor detector located behind the analyzer crystal (see ref 3, Figure 1). With the analyzer crystal "detuned" by ~100 arcsec from the Bragg angle, the transmission is given by the ratio of intensities, measured with and without sample.

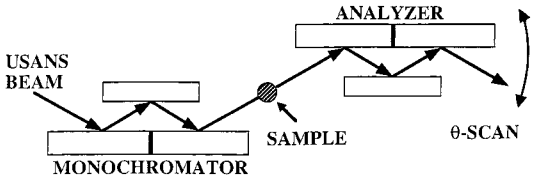

Figure 1. Schematic layout of USANS experiment: the analyzer is rotated to perform the θ-scan; scattering for the sample "spreads" the beam and is recorded as a broadened rocking curve.

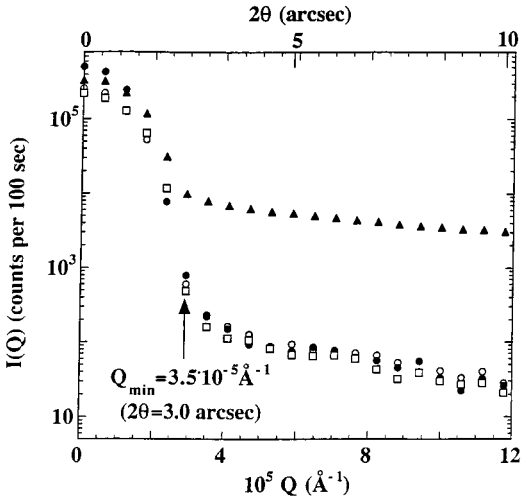

Figure 2. Raw rocking curves from HDPE/HPB (filled triangles), HDPE/LDPE (open circles), and LDPE-blank (open squares) polymer blends and from furnace with empty cell (filled circles) measured in the region $0 \le 2\theta \le 10$ arcsec.

In both SANS and USANS experiments, furnaces were used to keep polymer blends (contained in quartz cells) at a temperature 160 °C (above the melting point) and measure the scattering from the sample in the amorphous state. Because in the USANS measurements the windows of furnaces and sample cells generate a significant scattering background in addition to the background from the "empty" instrument, these components were measured separately and taken into consideration when data processing.

Results and Discussion

Figure 2 shows the rocking curves for the three polymer samples at 160 °C measured at the USANS facility in the angular range $0 < 2\theta < 10$ arcsec together with the rocking curve from the furnace/empty cell. It

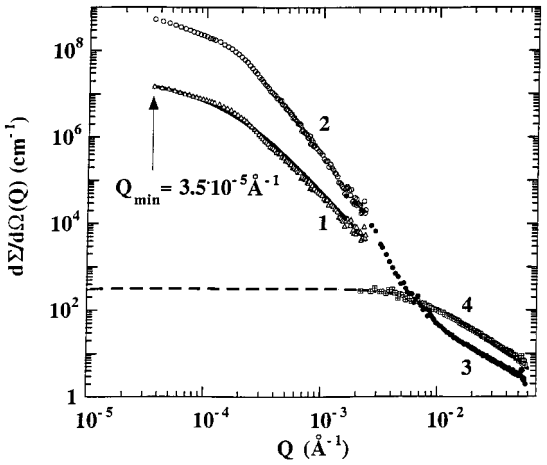

Figure 3. Combined SANS and USANS data from HDPE/HPB and HDPE/LDPE polymer blends. USANS experimental curve 1 from the HDPE/HPB sample is fitted to the Sabine−Bertram model (solid line) calculated for slit geometry. Curve 2 shows the same data transferred to point geometry by the Lake technique and overlapped with SANS data (curve 3) obtained at the 30m pinhole SANS instrument for the same HDPE/HPB blend. Curve 4 is SANS data collected from HDPE/LDPE sample fitted to the de Gennes RPA function (dashed line).

may be seen that the signal from the phase-separated HDPE/HPB blend (filled triangles) is clearly resolved and is orders of magnitude higher than the scattering from the HDPE/LDPE sample (open circles) and unlabeled LDPE "blank" (open squares). Moreover, the latter data are virtually superimposed, within the experimental scatter, on the signal produced by the windows of furnace and the empty cell (filled circles). Thus, the scattering cross section of these two samples is close to the detection limit ($\sim 10^3$ cm^{-1}) of current USANS instrumentation. After correcting for sample transmission, a small net signal is barely resolved beyond the experimental scatter for the HDPE/LDPE sample, but it is virtually the same for the LDPE blank, so it must arise from micrometer-size heterogeneities (catalyst residues, dirt, antioxidants, etc.), which are extrinsic to the blend morphology.[26] The scattering from the phase-separated HDPE/HPB blend is clearly resolved by USANS, despite the fact that the level of deuterium labeling is about 2.5 times lower than in the HDPE/LDPE blend. Had the latter sample been phase separated on micrometer-sized length scales, as asserted[2,5−7] previously, the cross section would have been well above the USANS scattering from the empty cell and have greatly exceeded the signal of the LDPE homopolymer blank. Similarly, the signal from the HDPE/HPB sample is much greater than that from the HDPE/LDPE blend, and if the scattering contrasts were similar, the concentration of any phase-separated aggregates of micrometer size would have to be orders of magnitude less than for the HDPE/HPB sample. Such a "dilute" morphology in the melt was not envisioned previously,[2,5−7] and thus these USANS results are consistent with the conclusions that the HDPE/HPB sample is phase separated in the melt and that the HDPE/LDPE blend is homogeneous, as previously indicated by pinhole SANS measurements.[1,4]

The conclusion is further reinforced by combining the USANS (curve 2) and pinhole SANS (curve 3) data from HDPE/HPB blend (Figure 3), though before this can be accomplished, corrections must be applied for instrumental resolution effects, which "smear" the scattering intensity over finite range of angles, $\Delta\theta$. In general, such effects are much smaller for SANS experiments than for USANS, because the former are taken with pinhole collimation, whereas USANS facilities use infinite slit geometry, where $\Delta\theta$, and hence the effect of smearing, is much larger. As $\Delta\theta$ is relatively independent θ, the angular uncertainty ($\Delta\theta/\theta$) is greater as $\theta \rightarrow 0$, so the effects of smearing are more pronounced at smaller angles. The main component of the distortion arises from the large range of angles ($\Delta\theta$) in the vertical plane, and the smearing effects are therefore very similar to those observed in long-slit Kratky cameras. Desmearing has been accomplished by a wide range of techniques, which have been reviewed by Glatter and Kratky,[27] and in this work the desmearing procedure was done by a simple iterative method due Lake[27,28] (see Appendix for the details). The various procedures are based on different assumptions, and as a cross check, an independent calculation was performed using the GNOM program developed by Svergun,[30] which reproduced the Lake-desmeared data within an accuracy ~10%. It will be seen below that the forward cross section [$d\Sigma/d\Omega(0) \sim 10^8$ cm^{-1}] of the desmeared data exceeds that of homogeneous blends by 6 orders of magnitude, and we therefore believe that this conclusion is independent of the method of desmearing.

As a plausible representation of the scattering from the inhomogenieties in the sample, we chose the model of a system of three-dimensional particles with different size and shape, recently developed by Sabine and Bertram,[31,32] which also accounts the effect of multiple scattering:

$$I(Q) \sim \sum_{10}^{n=1} (b^n/n^m)[1 + (1/n^m)(QR)^2]^{-2} \qquad (1)$$

where $m \cong 1.58$, the parameter b ($0 < b \leq 3$) is related to the average number of scattering events in the sample, and R is the average "radius" of particles.

One reason for choosing this model was that it was discovered experimentally that the scattering cross section from the HDPE/HPB blend depends on the sample thickness, thus indicating that the data contain a component of neutrons that have been scattered more than once (multiple scattering), which is only to be expected in view of the enormous forward scattering ($d\Sigma/d\Omega(0) \sim 10^8$ cm^{-1}). As the Sabine−Bertram model accounts for multiple scattering effects and gives an average domain radius ($R = 3.1$ μm) which is independent of the sample thickness (and hence multiple scattering effects), this indicates the self-consistency of the data treatment. The further details of multiple scattering and profile analysis will be given in a forthcoming publication.[32] The fact that the desmeared data (Figure 3) overlap smoothly with the independently calibrated pinhole SANS data, with no adjustable scale factors, forms an important cross check on the validity of the desmearing procedure.

The intensity of macromolecular scattering measured from the HDPE/LDPE sample by the 30m SANS facility is lower than the USANS detection limit ($\sim 10^3$ cm^{-1}), and thus the SANS scattering curve was extrapolated to the USANS region by fitting to the de Gennes random phase approximation, which has been widely used to describe partially deuterated homogeneous blends.[1,2,4] It may be seen that there is a dramatic difference

(approximately 6 orders of magnitude) between the zero-Q cross sections of the HDPE/HPB and HDPE/LDPE samples.

It is clear from the above results that USANS can clearly demonstrate phase separation on micrometer-sized length scales when present (e.g., for HDPE/HPB). The evidence that no such signal is detected from the HDPE/LDPE sample, despite the fact that the level of deuteration (25% instead of 10% for the HDPE/HPB blend) is higher, clearly shows that micrometer-sized phase-separated domains are not present in this blend. The signal from the HDPE/HPB sample is much greater than from the HDPE/LDPE blend, and if the scattering contrast factors were similar, the concentration of any phase-separated aggregates would have to much less than for the HDPE/HPB sample. Under the most optimistic assumption that in the HDPE/HPB blend the volume fraction of the dispersed phase was 50% and the domain size and concentration of linear and branched molecules within the phases were similar, then we can estimate that the maximum concentration of such phase-segregated aggregates in the HDPE/LDPE blend would be over 2 orders of magnitude less than for the HDPE/HPB blend (i.e., approximately 0.2%). Such a "dilute" morphology in the melt was not envisioned previously,[2,5−7] and this confirms conclusions derived from pinhole SANS experiments.[1,4] It is also consistent with recent Raman imaging studies,[33] which do not show evidence for liquid−liquid phase separation on HDPE/LDPE melts. While these are distinct differences in solid-state morphology of such blends when rapidly quenched from melt,[5−7,33] it does not appear that these arise from biphasic melts.

Acknowledgment. We acknowledge helpful discussions with D. I. Svergun (European Molecular Biology Laboratory, Germany). The research at Oak Ridge was supported by the Division of Material Sciences, U.S. Department of Energy, under Contract DE-AC5-96-OR22464 with Lockheed Martin Energy Research Corporation and in part by appointment to the Oak Ridge National Laboratory postdoctoral research associates program administered jointly by the Oak Ridge National Laboratory and the Oak Ridge Institute for Science and Education. The work at Florida State was supported by the National Science Foundation Polymer Program (DMR 94-19508).

Appendix

The scattering curve, $I(Q)$, defined in eq 1 is the theoretical intensity for point geometry, whereas the net experimental USANS scattering curve from the HDPE/HPB blend (Figure 3, curve 1) is measured in slit geometry. The fit (solid line) has been done for the net experimental scattering curve $I(Q)_{\text{slit/exp}}$ (curve 1) using the known convolution[29]

$$I(Q)_{\text{slit/th}} = \int\int W_{\text{h}}(t)\, W_{\text{v}}(u) I\{(2\pi/\lambda)[(2\theta - t)^2 + u^2]^{0.5}\}_{\text{point/th}}\, \mathrm{d}u\, \mathrm{d}t \quad (2)$$

where $I\{(2\pi/\lambda)[(2\theta - t)^2 + u^2]^{0.5}\}_{\text{point/th}}$ is in our case the Sabine−Bertram function $I(Q)$ [eq 1], $W_{\text{h}}(t)$ and $W_{\text{v}}(u)$ are horizontal and vertical collimation functions of the USANS instrument, respectively, t and u are the horizontal and vertical angular coordinates, and $W_{\text{h}}(t)$ and $W_{\text{v}}(u)$ obey the normalization condition:

$$\int W_{\text{h}}(t)\, \mathrm{d}t = \int W_{\text{v}}(u)\, \mathrm{d}u = 1 \quad (3)$$

$W_{\text{h}}(t)$ is the rocking curve of the empty USANS instrument, and $W_{\text{v}}(u)$ is the distribution of the primary beam intensity along the vertical axis of the detector plane, convoluted with the vertical aperture of the detector.[3]

The USANS data, collected in slit geometry (curve 1), were transferred to point geometry after fitting to a theoretical model by using the following relation:[28,29]

$$I(Q)_{\text{point}} = I(Q)_{\text{slit/exp}}\, I(Q)_{\text{point/th}}/I(Q)_{\text{slit/th}} \quad (4)$$

where $I(Q)_{\text{point}}$ is the desmeared intensity.

References and Notes

(1) Alamo, R. G.; et al. *Macromolecules* **1994**, *27*, 411.
(2) Schipp, C.; Hill, M. J.; Barham, P. J.; Cloke, V. M.; Higgins, J. S.; Oiazabal, L. *Polymer* **1996**, *37*, 2291.
(3) Agamalian, M.; Triolo, R.; Wignall, G. D. *J. Appl. Crystallogr.* **1997**, *30*, 345.
(4) Alamo, R. G.; Graessley, W. W.; Krishnamoorti, R.; Lohse, D. J.; Londono, D. J.; Mandelkern, L.; Stehling, F. C.; Wignall, G. D. *Macromolecules* **1997**, *30*, 561.
(5) Barham, P. J.; Hill, M. J.; Keller, A.; Rosney, C. C. A. *J. Mater. Sci. Lett.* **1988**, *7*, 1271.
(6) Hill, M. J.; Barham, P. J.; Keller, A.; Rosney, C. C. A. *Polymer* **1991**, *32*, 13/84.
(7) Hill, M. J.; Barham, P. J.; Keller, A. *Polymer* **1992**, *33*, 2530.
(8) Stehling, F. C.; Wignall, G. D. *Polym. Prepr., ACS Polym. Chem. Div.* **1983**, *24*, 211.
(9) Stein, R. S. NATO Workshop on Crystallization of Polymers, Mons, 1992.
(10) Wignall, G. D.; Londono, R. G.; Alamo, R. G.; Mandelkern, L.; Stehling, F. C. *Macromolecules* **1996**, *29*, 5332.
(11) Wignall, G. D.; Londono, R. G.; Lin, J. S.; Alamo, R. G.; Gallante, M. J.; Mandelkern, L. *Macromolecules* **1995**, *28*, 3156.
(12) Londono, J. D.; Narten, A. H.; Wignall, G. D.; Nonnell, K. G.; Hsieh, E. T.; Johnson, T. W.; Bates, F. S. *Macromolecules* **1994**, *27*, 2864.
(13) Krishnamoorti, R.; et al. *Macromolecules* **1994**, *27*, 3073.
(14) Graessley, W. W.; Krishnamoorti, R.; Balsara, N. P.; Fetters, L. J.; Lohse, D. J.; Schulz, D. N.; Sissano, J. A. *Macromolecules* **1993**, *26*, 1137.
(15) Nicholson, J. C.; et al. *Macromolecules* **1991**, *24*, 5665.
(16) Nesarikar, A.; Crist, B. *J. Polym. Sci.* **1994**, *B32*, 641.
(17) Tashiro, K.; et al. *Macromolecules* **1995**, *28*, 8484.
(18) Lohse, D. J. *Rubber Chem. Technol.* **1994**, *67*, 367.
(19) Wignall, G. D.; Bates, F. S. *Makromol. Chem.* **1988**, *15*, 105.
(20) Bates, F. S.; Wignall, G. D.; Koechler, W. C. *Phys. Rev. Lett.* **1985**, *55*, 2425.
(21) Bates, F. S.; Dierker, S. B.; Wignall, G. D. *Macromolecules* **1986**, *19*, 1938.
(22) Koechler, W. C. *Physica (Utrecht)* **1986**, *137B*, 320.
(23) Wignall, G. D.; Bates, F. S. *J. Appl. Crystallogr.* **1986**, *20*, 28.
(24) Dubner, W. S.; Schultz, J. M.; Wignall, G. D. *J. Appl. Crystallogr.* **1990**, *23*, 469.
(25) Hayashi, H.; Flory, P. J.; Wignall, G. D. *Macromolecules* **1983**, *16*, 1328.
(26) Renninger, A. L.; Wicks, G. G.; Uhlmann, D. R. *J. Polym. Sci., Polym. Phys. Ed.* **1975**, *13*, 1247.
(27) Glatter, O.; Kratky, O. *Small-Angle X-ray Scattering;* Academic Press: New York, 1982; p 128.
(28) Lake, J. A. *Acta Crystallogr.* **1967**, *23*, 191.
(29) Feigin, L. A.; Svergun, D. I. *Structural Analysis by X-ray and Neutron Scattering*; Plenum Press: New York, 1987.
(30) Svergun, D. I. *J. Appl. Crystallogr.* **1991**, *24*, 413.
(31) Sabine, T. M.; Bertram, W. K.; Aldrige, L. P. *Mater. Res. Soc. Proc.* **1995**, *376*, 499.
(32) Sabine, T. M.; Bertram, W. K. *Acta Crystallogr.*, in press.
(33) Hill, M. J.; Morgan, R. L.; Barham, P. *J. Polym. Mater. Sci. Eng.* **1998**, *78*, 76.

MA981091B